Available online at www.sciencedirect.com
SCIENCE DIRECT®
Bioorganic & Medicinal Chemistry 13 (2005) 3241–3248
Bioorganic & Medicinal Chemistry

Copper-metalated peptide palindrome derived from prion octarepeat: synthesis, aggregation, and oxidative transformations

C. Madhavaiah and Sandeep Verma*

Department of Chemistry, Indian Institute of Technology Kanpur, Kanpur 208016, India

Received 28 January 2005; revised 16 February 2005; accepted 16 February 2005
Available online 19 March 2005

Abstract—We report construction of a bis-pentapeptide conjugate **4** containing truncated pentapeptide sequence from prion octarepeats. Its copper-laden derivative **5** demonstrated a propensity for aggregate formation, which was studied by atomic force microscopy. Oxidative biochemical transformations catalyzed by **5** were evaluated by nucleic acid cleavage and by neurotransmitter oxidation, in the presence of external co-oxidants. Preliminary mechanistic analysis provides a hint for the involvement of reactive oxygen species in such transformations.

1. Introduction

Conformational changes in the normal cellular prion protein (PrP^C) to its aberrant isoform (PrP^{Sc}) results in several debilitating neurological diseases such as scrapie in sheeps, bovine spongiform encephalopathy (BSE) in cattle, Creutzfeldt–Jakob disease in humans.[1] PrP^C is a cuproglycoprotein, which binds copper through its N-terminal domain and is believed to play a significant role in copper homeostasis and metabolism.[2] C-terminal of PrP^C (126–231) is structured comprising of three α-helices and two β-strands, while the N-terminal is primarily unstructured as a random coil. Interestingly, a stretch of N-terminal (60–91) contains octapeptide repeat (PHGGGWGQ) that occurs four times consecutively and selectively binds Cu^{2+}, over other divalent metal ions, in a 1:1 stoichiometry.[3] The various roles attributed to the prion protein include its activity as periplasmic copper transporter, cellular reservoir, and stress sensor of copper ions and superoxide dismutase activity, to name a few.

Interaction of copper with truncated octarepeat peptide motifs were studied with the aid of spectroscopic methods to investigate the binding mode of copper in PrP^C.[3a,4] Recently, coordination mode of copper with HGGGW was established with single X-ray crystal structure.[5] The copper-bound octapeptide region of prion protein exhibits superoxide dismutase activity, thus serving as a possible defense system against oxidative stress in the brain.[6] PrP^C deficient mice were shown to be more sensitive toward oxidative stress, resulting in higher levels of oxidative damage to proteins and lipids.[7] Interestingly, nucleic acid damage was indirectly observed through the detection of oxidized nucleosides in brain section of patients affected with Creutzfeldt–Jakob disease.[8] In addition, the wild type prion protein affords efficient removal of copper from PC12 cell culture displaying a natural affinity for copper ions.[3c] Furthermore, copper-bound PrP_{23-98} induces carbonyl formation in dopamine and L-ascorbate indicating a wide manifestation of oxidative transformations.[9]

We recently reported fibrillogenesis of a novel bis-peptide scaffold based on the pentapeptide **PHGGG** derived from the prion octarepeat sequence.[10] This construct afforded amyloidogenic aggregation upon aging and the fibrils so formed were studied by multiple microscopic techniques. Herein, we wish to report synthesis and analysis of copper interaction with the bis-conjugate **4** [$(PHGGG)_2DAB$] by spectroscopic methods, followed by evaluation of its aggregational behavior and the oxidative transformations caused by the addition of an exogenous co-oxidant.

Keywords: Prion; Copper; Conjugate; Aggregation.
* Corresponding author. Tel.: +91 512 259 7643; fax: +91 512 259 7436; e-mail: sverma@iitk.ac.in

0968-0896/$ - see front matter © 2005 Elsevier Ltd. All rights reserved.
doi:10.1016/j.bmc.2005.02.029

2. Results and discussions

2.1. Synthesis and characterization

Pentapeptide **PHGGG** was used to synthesize a reverse bis-peptide conjugate by using a flexible 1,4-diaminobutane linker via routine solution-phase chemistry approaches, followed by its copper-metalation to yield **5**. All intermediates were thoroughly characterized by spectroscopic means (Scheme 1). Bis-pentapeptide **3** was deprotected and metalated with copper acetate monohydrate and characterized through ESI mass spectroscopy, UV–visible, and EPR. Subsequent to metalation, the amount of copper incorporated in the conjugate was determined from atomic absorption spectroscopy (AAS). This value was found to be 0.12 g of copper per gram of the conjugate and suggests stoichiometric presence of two copper atoms per bis-peptide conjugate. This corresponds to the binding of one copper ion to each pentapeptide half in the symmetrical metalated conjugate **4**.

We resorted to electrospray ionization mass spectroscopy (ESI-MS) to establish copper coordination pattern, due to lack of success in growing suitable crystals of **5** (Fig. 1). Soft ionizing-desorption technique, such as ESI-MS, allows for facile transfer and detection of intact metalated species. This technique is frequently used to provide accurate mass assignments for copper complexes by deciphering stoichiometric speciation. ESI-MS characterization of these complexes is in complete agreement of two-copper stoichiometry per bis-peptide.

In Fig. 1, high abundance *m*/*z* value with 512 indicates the monocopper centered fragment resulting from symmetrical rupture of dicopper-centered fragment, which was observed with *m*/*z* value of 1023 (1020+3H). However, ESI spectrum was recorded at pH 5.8, where the deprotonation of backbone amide is not possible. However in the fragmentation process, the so formed acetate counter anions, conjugate base of AcOH, could abstract protons from backbone amide thus making them appear

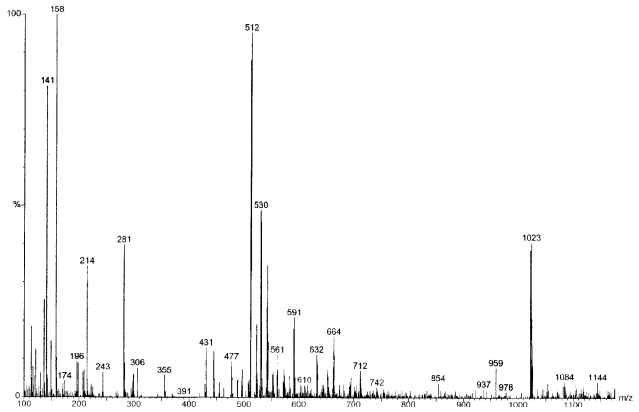

Figure 1. ESI-MS of copper metalated conjugate **5**.

in their deprotonated forms. Values of 1084, 1144 probably indicate the presence of two copper ions along with one or two acetate counter anions, respectively. Similar ESI mass spectral characterizations of copper binding to different positions of prion protein are reported.[4a,d,e] Interestingly we have not observed any *m*/*z* value representing an copper/peptide coordinated complex with 1:2 stoichiometry. Possible fragments formed in the ESI process of **5** are detailed in Scheme 2.

FT-IR spectra offers potentially useful information about metal ion–peptide interactions through shift in amide I and II frequencies. Therefore, we recorded IR spectra for the metal complex in order to monitor changes in coordination behavior with respect to unmetalated ligands. The following conclusions can be drawn from the spectral analysis:

- NH str bands appeared as broad peaks due to hygroscopic nature of the unmetalated conjugate **4**. These bands were observable in **5**, albiet with a lower frequency shift indicating that all amide nitrogens were possibly not deprotonated due to copper coordination.

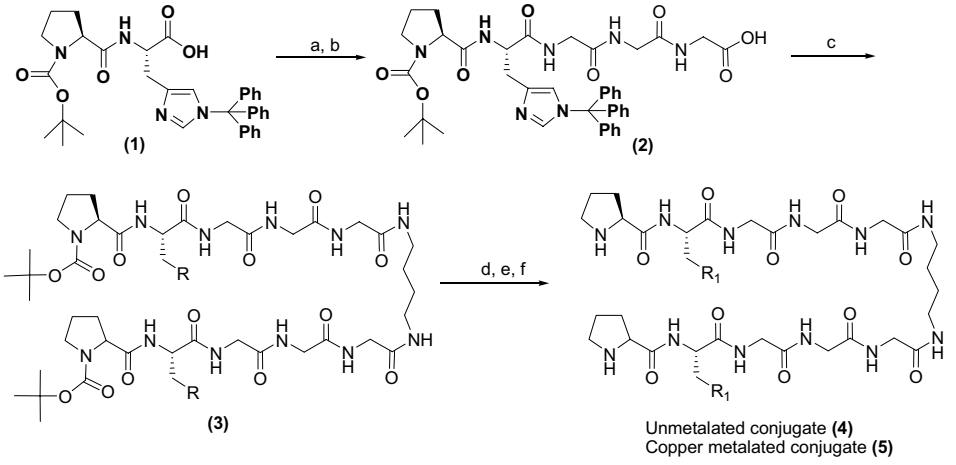

Scheme 1. Synthesis of copper metalated bis-conjugate **5**. Reagents and conditions: (a) HOBt, DCC, Cl−·+NH_3Gly-Gly-Gly-OMe, Et_3N, yield 81%; (b) 1 N NaOH, 1.5 h, rt, yield 100%; (c) HOBt, DCC, 1,4-diaminobutane, DCM, yield 61%; (d) 95% TFA, 3 h, rt, 80%; (e) strong anion exchange resin; (f) $Cu(OAc)_2{\cdot}H_2O$.

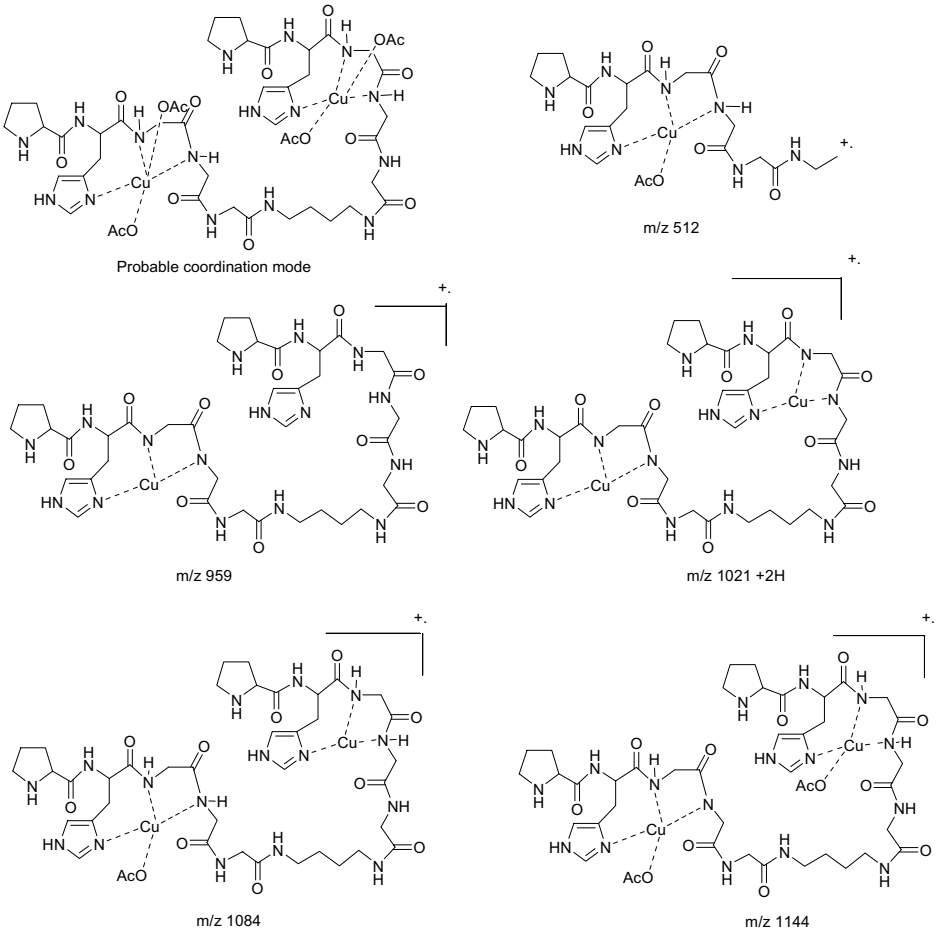

Scheme 2. Possible fragmentation of **5** in the ESI process.

- The amide I bond (–C═O str vibrations weakly coupled with C–N str and in-plane N–H bending) was not too much affected when compared to the unmetalated conjugate (for free conjugate 1656 cm^{-1} and for the metal conjugate 1660 cm^{-1}), thus suggesting lack of participation of backbone carbonyls in coordination.[11]
- The amide II (in-plane –NH bending strongly coupled with C–N str) band was considerably affected (for free conjugate 1542 cm^{-1}, for metal conjugate 1572 cm^{-1}), which clearly implicates participation of the backbone –NH in copper ion coordination in **5**.

UV–visible spectra for **5** were recorded in aqueous solutions, where λ_{max} was observed at 595 nm with an extinction coefficient of 116 M^{-1} cm^{-1}. EPR spectra for **5** was recorded at liquid nitrogen temperature in methanol (Fig. 2). The $g_{\|}$, $g_{\perp}$, $A_{\|}$, and $A_{\perp}$ values were 2.23, 1.99, 192 G, and 14, respectively.[4a] These values suggests for the presence of a square-based geometry around copper. It is documented that spectroscopic data with d–d transitions occur at 597 nm, while values of $g_{\|} = 2.23$ and $A_{\|} = 187$ G signify a 3 N species (NH, N^{-}, N^{im}) binding mode.[12a,b]

^{1}H NMR spectrum was recorded for **4**, in the presence or absence of copper. The addition of 1 equiv of copper chloride dihydrate influenced aromatic protons of the histidine side chain (Fig. 3). This observation suggests direct involvement of the histidine imidazole nitrogen in copper coordination. A similar observation was also reported with the octapeptide repeat (Ac-PHGGGWG-NH_2) in the presence of copper ions.[4c] Taken together, these results confirm involvement of two copper ions in conjugate **5** and each copper ion is predicted to coordinate via peptide backbone nitrogens and the imidazole nitrogens of the histidine side chain.

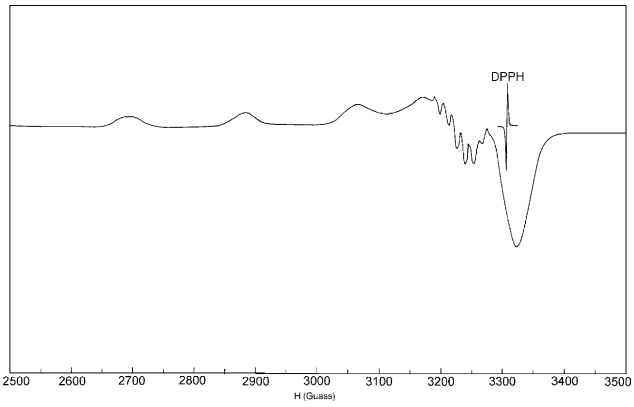

Figure 2. ESR spectra of **5**.

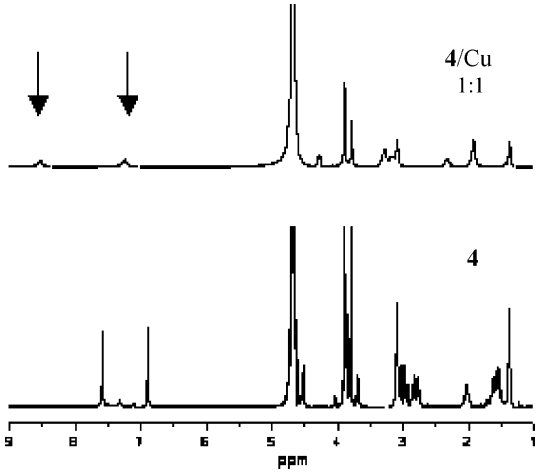

Figure 3. ^{1}H NMR experiment for copper interaction with **4**. Arrows indicate broadened signals belonging to the histidine aromatic protons.

It is not possible to predict the exact binding mode in the absence of the crystal structure of **5**.

2.2. Aggregation properties of copper metalated conjugate

It is evident from recent studies that copper affinity toward prion protein plays a crucial role in fibril formation. A study by Viles and co-workers demonstrated that copper can also bind to the unstructured region of the prion protein (90–120), outside the implicated domain of octarepeats.[4a] Interestingly, it was found that this binding not only occurs with nanomolar binding constant, but it also induces β-sheet like character subsequent to copper binding in an otherwise unstructured region. Such information may be pivotal in linking copper interaction to ordered aggregation of the prion protein.

We have studied the morphology of freshly prepared and 10 days aged solutions of **5** by AFM. Freshly prepared solution exhibited sparsely distributed punctated structures with 5 nm thickness (Fig. 4a). Upon aging for 10 days, an entirely different morphology was observed with the formation of aggregated clusters with a mean thickness of nearly 60 nm (Fig. 4b). Such accumulated aggregation are probably formed after aging for several days via the nucleation-seeding type of events. A similar pattern of fibrillogenesis leading to aggregation is similar to that observed with unmetalated conjugate **4** reported earlier by us.[10]

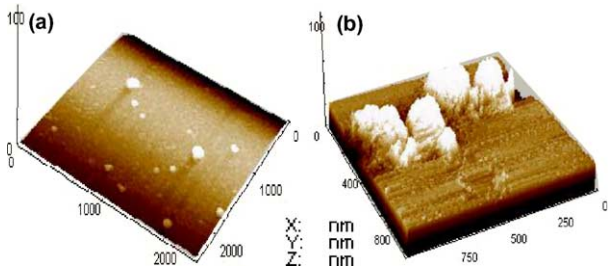

Figure 4. AFM micrographs of **5**: (a) freshly prepared; (b) 10 days aged.

2.3. Oxidative damage of pBR322 supercoiled DNA

Copper is an essential trace element, which may get inextricably involved in the pathophysiological stress owing to its aberrant homeostasis and/or excessive oxidant activity under hypoxic conditions.[13] Nucleic acids are convenient biomarkers to study oxidative stress and indeed enhanced nucleic acid damage was observed in the brain of patients suffering from Creutzfeldt–Jakob disease, a prion disorder.[8] This points toward possible generation of reactive oxygen species (radicals), which may eventually lead to neurodegeneration in prion disorders.

We have investigated possible generation of reactive oxygen species with **5** in presence of an exogenously added co-oxidant, by choosing supercoiled pBR322 DNA as a substrate. Copper–magnesium monoperoxyphthalate (MMPP) couple generates deleterious reactive oxygen, which interacts with the nucleic acid substrate. Time-course experiment revealed conversion of supercoiled DNA form **I** to its nicked form **III** in ~2 min by **5** (pH 7.5, 37 °C, Fig. 5a).

The nature of reactive species involved was probed by performing cleavage reactions in presence of hydroxyl radical scavengers such as D-mannitol, *tert*-butanol, and DMSO (Fig. 5b, lanes 3–5). Gel analysis clearly indicates involvement of diffusible hydroxyl radicals in cleavage reactions as all hydroxyl radical scavengers considerably inhibited cleavage reaction catalyzed by **5**. Presence of EDTA completely inhibited the reaction demonstrating a crucial role of coordinated copper for oxidative damage (Fig. 5b, lane 6). However, we were unsuccessful in direct detection of generated free radicals in order to provide an unequivocal proof of the proposed mechanism.

Cleavage reactions were further performed in presence of singlet oxygen quencher NaN_3, and enzymatic scavengers such as catalase and superoxide dismutase. NaN_3 afforded complete inhibition of the cleavage reaction (Fig. 6, lane 4), while catalase offered partial protection hinting at possible generation of hydrogen peroxide during the cleavage reaction (Fig. 6, lane 3). However, no effect was observed in the presence of SOD (Fig. 6, lane 2) indicating lack of involvement of superoxide radical anions in the cleavage reaction. It is worth to mention that these model reactions may simulate oxidative damage that can possibly occur in vivo through the generation of various reactive oxygen species in presence of

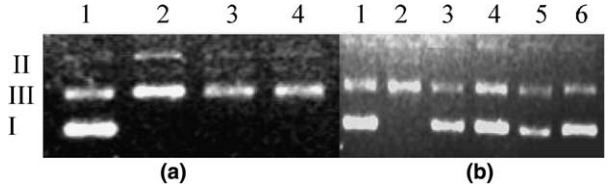

Figure 5. (a) pBR322 cleavage with **5**, time-course experiment: lane 1: DNA alone; Lanes 2–4: 1+MMPP+**5** (2, 4, 6 min, respectively); (b) scavenger experiments, 4 min reaction time: lane 1: DNA alone; lane 2: 1+MMPP+**5**; lanes 3–6: +DMSO; +*t*-BuOH; +D-mannitol; +EDTA.

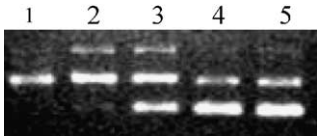

Figure 6. Enzymatic scavenger experiment for pBR322 cleavage by **5**+MMPP reaction. Lane 1: DNA+MMPP+**5**; lanes 2–4: +SOD; +catalase; +NaN_3; lane 5: DNA alone.

altered binding of copper to multiple folded/misfolded states of the prion protein.

2.4. Oxidation of dopamine and L-DOPA

Neurodegeneration caused by prion protein disorders have directed focus toward its role in maintaining copper homeostasis in presynaptic membranes as well as modulation of neuronal calcium ion levels, leading to an imbalance in synaptic transmission.[14] In fact, cellular isoform of prion protein *is* crucial for normal synaptic activity and loss of its function leads to synaptic malfunction and neuronal deterioration.[15] One study has reported prion protein directed control of monoamine oxidase activity leading to dopamine degradation,[16] while another related study has documented carbonyl formation on copper-bound $PrP_{23–98}$ in the presence of dopamine and ascorbate.[9]

With this background, we sought to analyze kinetics of oxidative degradation of dopamine and its biosynthetic precursor, L-DOPA with copper-laden conjugate **5**. Such experiment is akin to oxidative catabolism of neurotransmitters in the brain. Kinetic profiling was conducted using Lineweaver–Burk plots to estimate various kinetic parameters. As mechanistic analysis of plasmid cleavage showed in situ generation of H_2O_2, we decided to use it as a co-oxidant for neurotransmitter oxidation assay. It is important to mention that **5** alone did not yield oxidative transformations of dopamine and L-DOPA.

Similar to nucleic acid studies, incubation of **5** alone with dopamine hydrochloride did not give any oxidative products as determined by the appearance of *o*-diquinone-MBTH adduct in spectrophotometric assay. Subsequently, this reaction was activated by the addition of hydrogen peroxide and initial velocities were determined by measuring time-dependant formation dopamine-*o*-diquinone MBTH adduct at 505 nm (ε = 42.5 $mM^{-1}\,cm^{-1}$). Similar assay conditions were used for L-DOPA oxidation, where MBTH adduct of L-DOPA-*o*-diquinone was monitored at 500 nm (ε = 13.4 $mM^{-1}\,cm^{-1}$). Lineweaver–Burk plots were generated for both substrates to calculate maximal velocities (V_{max}), Michaelis-Menten constants (K_m) and turnover numbers (k_{cat}) (Figs. 7 and 8). For dopamine, K_m, V_{max}, and k_{cat} were found to be 0.25 mM, 6.52×10^{-3} mM min^{-1}, and 65.91×10^{-3} min^{-1}, respectively. These values for L-DOPA oxidation were 0.14 mM, 3.33×10^{-3} mM min^{-1}, and 33.16×10^{-3} min^{-1}, respectively.

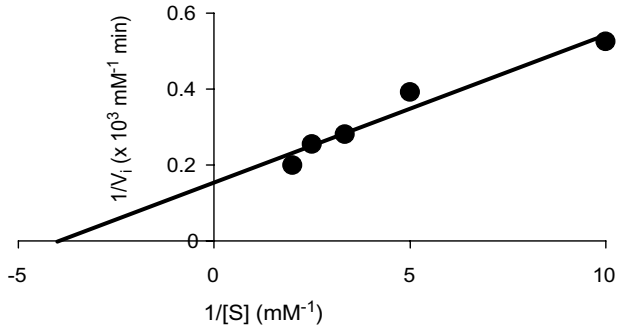

Figure 7. Lineweaver–Burk plot for dopamine oxidation catalyzed by **5**.

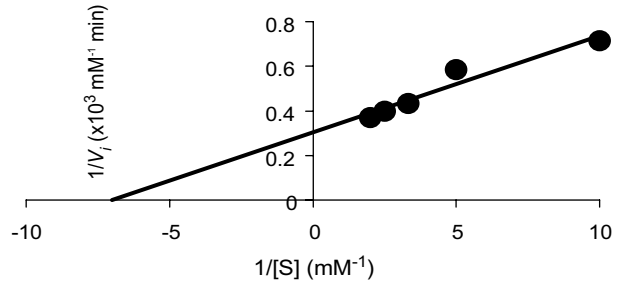

Figure 8. Lineweaver–Burk plot for L-DOPA oxidation catalyzed by **5**.

These results confirm the possibility of oxidative destruction of neurotransmitters by copper-metalated prion protein causing malfunction in synpatic transmission, leading to various pathophysiological states of prion disorders. Although the precise mechanism of neurodegeneration by PrP^{Sc} is far from resolved,[17] it is possible that copper-laden PrP^{C} or interaction of free copper with PrP^{Sc}, under oxygen-rich environment, may lead to the depletion of released neurotransmitters, thus affecting normal brain function.

3. Conclusions

Recent investigations into the role of copper binding to prion protein have drawn considerable attention. A report by Viles and co-workers elegantly demonstrate the ability of copper coordination to induce β-sheet character to the unstructured region of the prion protein, raising the possibility of copper acting as a trigger for prion misfolding.[4a] Such observations will require reinvestigation of the role of copper in prion aggregation and ensuing neurotoxicity, necessitating construction of newer model peptides, which are able to model prion–copper interaction.

In this vein, this report describes crafting of a novel copper metalated reverse bis-peptide conjugate **5** derived from truncated octarepeats located in the N-terminal of the prion protein. Copper metalated conjugate was characterized by employing UV–vis, atomic absorption, electron paramagnetic resonance, ESI-MS, and IR

spectroscopic techniques. Copper ions in the conjugate are proposed to coordinate through backbone amide nitrogens along with imidazole nitrogens of the histidine side chain on the basis on preliminary spectroscopic investigations. Aging studies with **5** revealed formation of plaque-like structures. Bis-conjugate design elegantly combines the structural elements of two octarepeat monomeric units to give optimal copper binding motif and coincidentally, another investigation has demonstrated that octarepeat dimer and tetramer are more effective copper binding ligands compared to a simple monomer.[18]

The oxidative properties of **5**, in presence of MMPP or H_2O_2 as co-oxdiants, were evaluated by employing supercoiled DNA, dihydroxy substrates dopamine hydrochloride and dopamine. Compound **5** exhibited remarkable cleavage activity in presence of an external co-oxidant. Preliminary mechanistic investigations revealed a definite involvement of reactive oxygen species, most likely hydroxyl radicals, in the cleavage reactions. Thorough kinetic profiling of neurotransmitter oxidation suggests that such a model system can be used to ascertain the mechanism of oxidative damage of essential biomolecules such as nucleic acid bases and lipids, and work toward this end is currently under progress.

4. Experimental

4.1. Spectral analyses

^1H, ^{13}C NMR spectra were recorded on a JEOL-JNM LAMBDA 400 model operating at 400 or 100 MHz, respectively. IR spectra were recorded on a Bruker FT-IR Vector 22 model from 4000–400 cm^{-1} in the KBr pellet form. UV–visible spectra were recorded on Shimadzu UV-160 model spectrophotometer. FAB mass spectra were recorded on a JEOL SX-120/DA6000 spectrometer using argon (6 kV, 10 mA) as the FAB gas, at Sophisticated Analytical Instrumentation Facility, CDRI, Lucknow. The accelerating voltage was 10 kV and the spectra were recorded at room temperature and *m*-nitrobenzyl alcohol or glycerol was used as the matrix. The electrospray ionization mass (ESI-MS) spectra were recorded on a MICROMASS QUATTRO II triple quadrupole mass spectrometer. EPR spectra was recorded on a Varian spectrometer at the X-band frequency and the magnetic field strength was calibrated using DPPH ($g = 2.0036$). The amount of metal present in peptide conjugate was estimated by using atomic absorption spectroscopy (GBC).

4.2. Chemicals and reagents

N,*N*′-Dicyclohexylcarbodiimide and $Cu(OAc)_2{\cdot}H_2O$ (Lancaster), triethylamine, trifluoroacetic acid, ethidium bromide (SRL, India). *N*-Hydroxybenzotriazole and 1,4-diaminobutane were purchased from Fluka (Switzerland). The dipeptide *tert*-butyloxycarbonyl-L-prolyl-N^{im}(trityl)-L-histidine (**1**) and the pentapeptide *tert*-butyloxycarbonyl-L-prolyl-N^{im}(trityl)-L-histidyl-glycyl-glycyl-glycine (**2**) were synthesized by using solution phase methods. Supercoiled pBR322 DNA was purchased from Bangalore Genei Pvt. Ltd. Strong anion exchange resin (Dowex 1-X8) was from J. T. Baker chemical company. L-Dopa and dopamine hydrochloride were purchased from Spectrochem, India. NMR spectra were recorded in DMSO-d_6 (Aldrich) or in D_2O. FAB MS and ESI-MS were recorded at RSIC, Lucknow and AAS values were recorded at FEAT Laboratory, IIT-Kanpur.

4.3. Synthesis and characterization of peptide conjugates (3–5)

4.3.1. *N*,*N*′-Bis-(*t*-butoxycoarbonyl-L-prolyl-N^{im}(trityl)-L-histidyl-glycyl-glycyl-glycine)-1,4-diaminobutane (3). This conjugate was synthesized as reported in our previous communication.[10] HOBt (0.648 g, 4.8 mmol, 1 equiv) was added to a pre-cooled solution of *t*-butoxycarbonyl-L-prolyl-N^{im} (trityl)-L-histidyl-glycyl-glycyl-glycine (3.66 g, 4.8 mmol, 1 equiv) in anhydrous dichloromethane (55 mL). DCC (1.10 g, 5.28 mmol, 1.1 equiv) in dry DCM (1 mL) was added drop-wise to the peptide solution with constant stirring. Stirring was continued for 10 min at 0 °C and then for 50 min at room temperature. After this time, 1,4-diaminobutane (0.24 mL, 2.35 mmol, 0.5 equiv) in dry DCM (0.2 mL) was added drop-wise at room temperature with constant stirring and it was continued for 20 h. The precipitated dicyclohexylurea was filtered off after this time and washed with dichloromethane (4×5 mL). Combined organic layers were washed with 2 N HCl (3×40 mL), 10% $NaHCO_3$ (3×40 mL) and finally with saturated brine solution and dried over anhydrous Na_2SO_4. Solvent was evaporated under reduced pressure and the crude product was purified by silica gel column using dichloromethane/methanol (93:7) to afford pure fully protected conjugates. [R_f 0.6 (6% methanol in DCM), yield 61% (2.3 g), mp = 141–143 °C, $[\alpha]_D^{25}$ −28 (*c* 1 in methanol, 25 °C), FAB MS (M+3) = 1585].

^1H NMR: (400 MHz, [D]$CHCl_3$, 25 °C, TMS) $\delta = 1.16$ (s, 18H, ^{t}Boc); 1.44 (br s, 4H, Linker's $-CH_2CH_2$); 1.93 (m, 4H, Pro γH); 2.24 (appeared as br s, 4H, Pro βH); 2.84–2.886 (dd, J(H,H) = 4.8 Hz and 10.2 Hz, 2H, His βH); 3.06–3.13 (br dd, 6H, overlapping signals for His βH and Linkers $-CH_2N$); 3.41–3.45 (m, 4H, overlapping signal for Pro δH and Gly $-CH_2$); 3.53–3.58 (dd, J(H,H) = 6.4 Hz and 11.6 Hz, 2H, Pro δH); 3.69–3.84 (m, 6H, overlapping signals of Gly CH_2); 3.90–3.96 (dd, J(H,H) = 5.2 Hz and 17.2 Hz, 2H, Gly $-CH_2$); 4.05–4.08 (dd, J(H,H) = 4.8 Hz and 8.0 Hz, 2H, Pro αH); 4.13–4.19 (dd, J(H,H) = 7.2 Hz and 17.2 Hz, 2H, Gly $-CH_2$); 4.46–4.50 (q, J(H,H) = 5.2 Hz, 2H, His αH); 6.56 (s, 2H, His ring's H); 6.97 (br d, 12H, Ar C–H); 7.24–7.29 (m, 24H, overlapping signals for Ar C–H, His ring's C–H and –NH); 7.39 (br s, 2H, –NH); 7.70 (br s, 4H, –NH); 9.04 (d, J(H,H) = 6.6 Hz, 2H, –NH). ^{13}C (100 MHz, [D] $CHCl_3$, 25 °C, TMS) $\delta = 24.72$, 26.31, 27.73, 28.36, 30.2, 38.92, 43.14, 43.19, 43.32, 47.24, 54.37, 61.88, 75.59, 81.22, 120.53, 128.16, 128.37, 129.66, 136.15, 138.24, 141.90, 156.36, 169.29, 169.95, 170.37, 172.53, 174.79.

4.3.2. *N*,*N*′-Bis-(L-prolyl-L-histidyl-glycyl-glycyl-glycine)-1,4-diaminobutane (4). A mixture of trifluoroacetic acid (95%) in dichloromethane (12 mL) was added to conjugate protected conjugate (2.0 g, 1.3 mmol), at room temperature with constant stirring under calcium filled guard-tube protection. Stirring was continued for 3 h at room temperature. After this time, the solvent was evaporated under reduced pressure and resulting residue was triturated with diethyl ether. The white solid so formed was washed with dichloromethane to yield the peptide (1.54 g) as its trifluoroacetate salt. This was passed through strong anion exchange resin (Dowex 1-X8, J. T. Baker, USA) and eluted with 50% aqueous methanol, followed by recrystallization from cold isopropyl alcohol and diethyl ether to give **4**. R_f (methanol/acetic acid/water = 1:0.25:0.42) = 0.35, yield = 80%, mp = 193–195 °C, $[\alpha]_D^{25}$ −18 (*c* 1 in methanol, 25 °C), FAB MS (M+2) = 900.

^{1}H NMR (400 MHz, [D]H_2O, 25 °C, TMS) δ = 1.35 (br s, 4H, Linker's –CH_2CH_2); 1.47–1.63 (m, 6H, Pro γ, βH); 1.95 (m, 2H, Pro βH); 2.72–2.84 (m, 4H, His βH); 2.90–3.06 (m, 6H, overlapping signals for linker's –CH_2NH and Pro δH); 3.23 (appeared as br t, 2H, Pro δH); 3.63–3.67 (dd, *J*(H,H) = 5.2 Hz and 8.4 Hz, 2H, His αH); 3.76 (br s, 4H, Gly –CH_2); 3.84 (d, *J*(H,H) = 5.2 Hz, 4H, Gly –CH_2); 3.869 (br s, 4H, Gly –CH_2); 4.47–4.51 (dd, *J*(H,H) = 6.4 Hz and 8 Hz, 2H, Pro αH); 6.87 (s, 2H, His ring's H); 7.56 (s, 2H, His ring's H). ^{13}C (100 MHz, [D]H_2O, 25 °C) δ = 25.68, 26.43, 30.17, 38.20, 41.98, 42.19, 42.59, 46.48, 51.85, 60.08, 127.52, 127.25, 135.25, 168.46, 169.81, 171.49, 174.18.

4.3.3. Metalation of bis-peptide conjugate (5). Peptide conjugate was treated with 2 equiv of copper acetate monohydrate in 50% aqueous methanol for 6 h at room temperature. After this time, the solvent was evaporated under reduced pressure. The residue was washed with hot 1,4-dioxane, acetone and then dried in vacuo. Metalated peptide conjugate was characterized through EPR, UV–visible spectra. The amount of copper present in the peptide conjugate was determined by atomic absorption spectroscopic measurements.

The electrospray ionization mass (ESI-MS) spectra of **5** were recorded on a MICROMASS QUATTRO II triple quadrupole mass spectrometer. Copper metalated **4** was dissolved in water (pH 5.8), which was subsequently introduced into the ESI source through a syringe pump at the rate of 5 μL per min. The ESI capillary was set at 3.5 kV and the cone voltage was 40 V. The spectra were collected in 6 s scans and the print outs are averaged spectra of 6–8 scans.

4.4. General experimental procedures

4.4.1. Anion exchange column. Strong anion exchange resin (Dowex 1-X8) was washed with three column volumes (3 × 30 mL) of 0.5 N NaOH prepared in 80% of aqueous dioxane, followed by three column volumes of 0.1 N NaOH. Then the column was washed with water until the washings showed the neutral pH (pH 7.0). Then the hydrochloride salts of **4** was dissolved in water and passed through the column. The column was washed with aqueous water, washings are combined, and evaporated to give **4** as its free amine.

4.4.2. NMR titration of copper binding to 4. Compound **4** (4.5 mg, 5 μmol) was dissolved in D_2O (0.56 mL, 99% atom D) to give a 9 mM solution. Increasing amounts of $CuCl_2{\cdot}2H_2O$ was added (0.25, 0.75, or 1.12 mg) and ^{1}H NMR spectra was recorded in D_2O on a JEOL-JNM LAMBDA 400 model operated at on a JEOL-JNM LAMBDA 400 model operated at 400 MHz, after a 10 min incubation at room temperature.

4.4.3. IR, UV–vis, and EPR spectroscopy. Spectra were recorded on a Bruker FT-IR Vector 22 model from 4000–400 cm^{-1} in the KBr pellet form. UV–visible spectroscopic studies were carried in methanol (pH 5.8) by using Shimadzu UV-160 spectrophotometer. EPR spectrum was recorded on a Varian spectrometer at X-band frequency and the magnetic field strength was calibrated using DPPH (*g* = 2.0036). The preformed 1:2 (conjugate/copper) copper complex of conjugate 4 was dissolved in methanol and EPR spectrum was recorded at liquid nitrogen temperature at pH 5.8.

4.4.4. Atomic force microscopy. Compound **5** (1 mM) was aged in 50% aqueous trifluoroethanol for 10 days or as fresh sample for AFM imaging. Peptide solution was sonicated (30 s) and dispersed on freshly cleaved mica followed by drying under nitrogen flow. The samples were imaged with an atomic force microscope (Molecular Imaging, USA), operated in Acoustic AC mode (AAC) with the aid of a cantilever (NSC12(c), MikroMasch). The force constant was 0.6 N/m, while the resonant frequency used was 150 kHz. The images were taken in air at room temperature, with a scan speed of 1.5–2.2 lines/s. Data acquisition was performed by PicoScan 5 software and the analysis was done with the aid of visual SPM.

4.4.5. pBR322 oxidative cleavage experiment. All supercoiled DNA modification reactions were performed in sodium cacodylate buffer at pH 7.5, at 37 °C, unless otherwise mentioned, in the presence of MMPP. Total reaction volume was 20 μL. The final concentrations of **5** and MMPP were 100 μM and weight of the DNA used was 16 ng/μL. For scavenger assay, weight of the DNA was 14 ng/μL, and concentration of scavengers was 100 mM. All reactions were quenched with 5 μL of loading buffer contains 100 mM of EDTA, 50% glycerol in Tris–HCl, pH 8.0 and the samples were loaded onto 0.7% of agarose gel containing ethidium bromide (1 μg/mL). Finally gels were imaged on PC-interfaced Bio-Rad Gel Documentation System 2000.

4.4.6. Dopamine and L-DOPA oxidation. Oxidation reactions were performed in 0.01 M *N*-ethylmorpholine buffer (pH 7.5; *T* = 30 °C) prepared in 80% aqueous methanol. Total reaction volume was 1.2 mL, contains 0.01 mL of hydrogen peroxide (30% w/v), 1 mL of appropriate concentration of substrate, 0.1 mL of MBTH, and 0.09 mL of bis-pentapeptide copper

complex. Final concentration of **5** was 0.1 mM and concentration range of L-dopa and dopamine was 0.1–0.5 mM. Oxidation products, L-dopa-*o*-diquinone and dopamine-*o*-diquinone were trapped with MBTH and the resultant adducts were monitored at 500 nm ($\varepsilon = 13.4\ mM^{-1}\ cm^{-1}$) and 505 nm ($42.5\ mM^{-1}\ cm^{-1}$), respectively.

Acknowledgements

C.M. thanks Council for Scientific and Industrial Research (CSIR) for award of a SRF. This work was partially supported by funds from the Department of Science and Technology, India, to one of us (S.V.).

References and notes

1. (a) May, B. C.; Govaerts, C.; Prusiner, S. B.; Cohen, F. B. *Trends Biochem. Sci.* **2004**, *29*, 162; (b) Ross, C. A.; Poirier, M. A. *Nature Med.* **2004**, *10*, S10; (c) Chesebro, B. *Br. Med. Bull.* **2003**, *66*, 1.
2. (a) Klamt, F.; Dal-Pizzol, F.; Frota, M. L. C.; Walz, R.; Andrades, M. E.; Da Silva, E. G.; Brentani, R. R.; Izquierdo, I.; Moreira, J. C. F. *Free Radical Biol. Med.* **2001**, *30*, 1137; (b) Pauly, P. C.; Harris, D. A. *J. Biol. Chem.* **1998**, *273*, 33107; (c) Brown, D. R.; Schmidt, B.; Kretzschmar, H. A. *J. Neurochem.* **1998**, *70*, 1686; (d) Brown, D. R.; Qin, K.; Herms, J. W.; Madlung, A.; Manson, J.; Strome, R.; Fraser, P. E.; Kruck, T.; Von Bohlen, A.; Schulz-Schaeffer, W.; Giese, A.; Westway, D.; Kretzschmar, H. *Nature* **1997**, *390*, 684.
3. (a) Millhauser, G. L. *Acc. Chem. Res.* **2004**, *37*, 79; (b) Stöckel, J.; Safar, J.; Wallace, A. C.; Cohen, F. E.; Prusiner, S. B. *Biochemistry* **1998**, *37*, 7185; (c) Miura, T.; Hori-I, A.; Takeuchi, H. *FEBS Lett.* **1996**, *396*, 248.
4. (a) Jones, C. E.; Abdelraheim, S. R.; Brown, D. R.; Viles, J. H. *J. Biol. Chem.* **2004**, *279*, 32018; (b) Brown, D. R.; Guantieri, V.; Grasso, G.; Impellizeri, G.; Pappalardo, G.; Rizzarelli, E. *J. Inorg. Biochem.* **2004**, *98*, 133; (c) Shields, S. B.; Franklin, S. J. *Biochemistry* **2004**, *43*, 16086; (d) Luczkowski, M.; Wiśniewska, K.; Lankiesicz, L.; Kozlowski, H. *J. Chem. Soc., Dalton Trans.* **2002**, 2266; (e) Luczkowski, M.; Kozlowski, H.; Stawikowski, M.; Rolka, K.; Gaggelli, E.; Valensin, D.; Valensin, G. *J. Chem. Soc., Dalton Trans.* **2002**, 2269; (f) Whittal, R. M.; Ball, H. L.; Cohen, F. E.; Burlingame, A. L.; Prusiner, S. B.; Baldwin, M. A. *Protein Sci.* **2000**, *9*, 332; (g) Bonomo, R. P.; Impellizzeri, G.; Pappalardo, G.; Rizzarelli, E.; Tabbı, G. *Chem. Eur. J.* **2000**, *6*, 4195; (h) Viles, J. H.; Cohen, F. E.; Prusiner, S. B.; Goodin, D. B.; Wright, P. E.; Dyson, H. J. *Proc. Natl. Acad. Sci. U.S.A.* **1999**, *96*, 2042; (i) Miura, T.; Hori, A.; Mototani, H.; Takeuchi, H. *Biochemistry* **1999**, *38*, 11560.
5. Burns, C. S.; Aronoff-Spencer, E.; Munham, C. M.; Lario, P.; Avdievich, N. I.; Antholine, W. E.; Olmstead, M. M.; Vrielink, A.; Gerfen, G. J.; Peisach, J.; Scott, W. G.; Millhauser, G. L. *Biochemistry* **2002**, *41*, 3991.
6. (a) Brown, D. R.; Clive, C.; Haswell, S. J. *J. Neurochem.* **2001**, *76*, 69; (b) Brown, D. R.; Wong, B. S.; Hafiz, F.; Clive, C.; Haswell, S.; Jones, I. M. *Biochem. J.* **1999**, *344*, 1.
7. Wong, B. S.; Liu, T.; Li, R.; Pan, T.; Petersen, R. B.; Smith, M. A.; Gambetti, P.; Perry, G.; Manson, J. C.; Brown, D. R.; Sy, M. S. *J. Neurochem.* **2001**, *76*, 565.
8. Guentchev, M.; Siedlak, S. L.; Jarius, C.; Tagliavini, F.; Castellani, R. J.; Perry, G.; Smith, M. A.; Budka, H. *Neurobiol. Dis.* **2002**, *9*, 275.
9. Shiraishi, N.; Nishikimi, M. *FEBS Lett.* **2002**, *511*, 118.
10. Madhavaiah, C.; Verma, S. *Chem. Commun.* **2004**, 638.
11. Facchin, G.; Torre, M. H.; Kremer, E.; Piro, O. E.; Castellano, E. E.; Baran, E. J. *J. Inorg. Biochem.* **2002**, *89*, 174, and references cited therein.
12. (a) Kozlowski, H.; Bal, W.; Dyba, M.; Kowalik-Jankowska, T. *Coord. Chem. Rev.* **1999**, *184*, 319; (b) Pettit, L. D.; Gregor, J. E.; Kozlowski, H. In *Perspectives on Bioinorganic Chemistry*; Hay, R. W., Dilworth, J. R., Nolan, K. B., Eds.; JAI: London, 1991; p 1.
13. Harris, E. D. *Annu. Rev. Nutr.* **2000**, *20*, 291.
14. (a) Vassallo, N.; Herms, J. *J. Neurochem.* **2003**, *86*, 538; (b) Brown, D. R. *Trends Neurosci.* **2001**, *24*, 85.
15. Collinge, J.; Whittingtone, M. A.; Sidle, K. C. L.; Smith, C. J.; Palmer, M. S.; Klarke, A. R.; Jefferys, J. G. R. *Nature* **1994**, *370*, 295.
16. Lee, H.-G.; Park, S.-J.; Choi, E.-K.; Carp, R. I.; Kim, Y.-S. *J. Mol. Neurosci.* **1999**, *13*, 121.
17. Castilla, J.; Hetz, C.; Soto, C. *Curr. Mol. Med.* **2004**, *4*, 397.
18. Valensin, D.; Luczkowski, M.; Mancini, F. M.; Legowska, A.; Gaggelli, E.; Valensin, G.; Rolka, K.; Kozlowski, H. *Dalton Trans.* **2004**, 1284.